



## Neutron in situ crystallization studies of Ti-based BMGs

J.L. Soubeyroux<sup>a,\*</sup>, J.N. Mei<sup>a,b</sup>

<sup>a</sup> Institut Néel/CRETA, CNRS Grenoble, 25 Avenue des Martyrs, BP 166, 38042 Grenoble Cedex 9, France

<sup>b</sup> State Key Laboratory of Solidification Processing, Northwestern Polytechnical University, Xi'an, 710072, Shaanxi, PR China

### ARTICLE INFO

#### Article history:

Received 20 July 2009

Received in revised form 18 February 2010

Accepted 7 April 2010

Available online 28 April 2010

#### Keywords:

Bulk metallic glass

Crystallization

Neutron diffraction

### ABSTRACT

The phase evolution upon heating of  $\text{Ti}_{40}\text{Zr}_{25}\text{Cu}_9\text{Ni}_8\text{Be}_{18}$  BMG was investigated by in situ neutron diffraction studies and compared to Differential scanning calorimetry measurements performed at the same heating rate. When the experiment is performed at the constant speed of 2 K/min, the amorphous to crystallization process proceeds by two complicated crystallization reactions: firstly, the precipitation of a cubic  $\text{Ti}(\text{Zr})\text{Be}_2$  phase at 608 K ( $a = 6.603 \text{ \AA}$ ), this phase then disappears at 810 K, secondly, by the formation at 749 K of two phases which have been determined by neutron diffraction to be a C14 hexagonal Laves phase and a big cube  $(\text{Zr},\text{Ti})_2\text{Ni}$  phase. When the sample is heated at 2 K/min, then hold at  $T_g + 158 = 713 \text{ K}$  (before  $T_{x2} = 749 \text{ K}$ ) the  $(\text{Ti},\text{Zr})\text{Be}_2$  phase develops. After 60 min, the big cube phase starts to appear, an important amorphous bump being still present. These in situ diffraction experiments and the different phases formed are presented and discussed.

© 2010 Elsevier B.V. All rights reserved.

### 1. Introduction

Much attention is actually paid to find and to study Ti-based bulk metallic glasses (BMGs) due to their high specific strength, low weight and low cost [1–8]. Development of these BMGs can expand the field of their applications. Recently, Kim et al. [9] have discovered a new phase ( $\text{Ti}_{40}\text{Zr}_{25}\text{Ni}_8\text{Cu}_9\text{Be}_{18}$ ) with high glass forming ability (GFA), high Young modulus and high plasticity at room temperature (7%). Enhanced plasticity has been discovered in formulas in the vicinity of this composition [10] and the authors have noticed that the first crystallization product can play an important role. They propose that when this first crystallization product is an icosahedral phase (i-phase), the plasticity is enhanced, while it is reduced when first crystallization product is a crystalline phase such as  $\alpha\text{-Ti}$  or  $\text{Ti}_2\text{Cu}$ . In a previous study [11], we have added Nb to this BMG to form  $(\text{Ti}_{40}\text{Zr}_{25}\text{Ni}_8\text{Cu}_9\text{Be}_{18})_{100-x}\text{Nb}_x$  ( $x = 0, 3, 5, 8, 10 \text{ at.}\%$ ) alloys and we have shown that low Nb addition content increases the formation of i-phase ( $\text{Nb}_x = 3$  or 5%), while more Nb addition was ineffective. Extensive studies on the kinetics behavior of the master compound under isochronal crystallization [12–14] or under compression [15] have been done, whereas the phase formation during crystallization, which is an important parameter, is not well understood. In Refs. [9,14], it is mentioned that at an annealing temperature  $T = 753 \text{ K}$  or  $680 \text{ K}$ , an i-phase is present, while at  $T = 873 \text{ K}$  or  $800 \text{ K}$ , only a Laves phase is present. These observations have been made by X-ray diffraction after annealing

and cooling the samples at various temperatures. In this article we present the results obtained by in situ neutron diffraction on amorphous bulk samples and compared with DSC studies performed at the same speed than the neutron diffraction study. Annealing at low temperature has also been observed by in situ neutron diffraction. Electron microscopy's analysis (SEM and TEM equipped with energy-dispersive X-ray spectrometry (EDS)) has been used to characterize the samples before and after annealing steps.

### 2. Experimental procedure

Ingots with nominal composition  $\text{Ti}_{40}\text{Zr}_{25}\text{Ni}_8\text{Cu}_9\text{Be}_{18}$  were prepared by HF-melting the mixture of the pure Ti, Zr, Cu, Ni and Be elements in a copper cold crucible. Bulk alloys in a cylindrical form with 40 mm in length and 3 mm in diameter were prepared by injection method in a copper mould under argon gas. The phase components and microstructure were obtained by scanning electron microscopy (SEM) (JEOL-5600LV equipped for EDS) and Transmission Electron Microscopy (TEM) (TECNAI F30 equipped for EDS). Thermal properties were measured by differential scanning calorimetry (DSC) (NETZSCH DSC 404S) at a heating rate of 2 K/min under flowing argon gas in order to be compared with neutron experiments and at 10 K/min. In situ neutron diffraction was studied on the D1B-CRG diffractometer at Institute Laue Langevin in Grenoble at the 2.518 Å wavelength, spectra during continuous heating at 2 K/min under vacuum were recorded every 5 min using a position sensitive detector covering  $80^\circ$  in  $2\theta$ . The sample was heated in the bulk form and during the heating treatment was continuously under high secondary vacuum, so that no oxidation mechanism could interfere with crystallization. Post-mortem X-ray diffraction studies have also been performed on the samples after neutron diffraction experiments. Data reduction was done with the LAMP and FULLPROF programs of ILL [16].

### 3. Results and discussion

Table 1 reports the results of thermal analysis obtained from the DSC experiments performed at different speeds and compared with

\* Corresponding author. Tel.: +33 476889039; fax: +33 476881280.

E-mail address: [jean-louis.soubeyroux@grenoble.cnrs.fr](mailto:jean-louis.soubeyroux@grenoble.cnrs.fr) (J.L. Soubeyroux).

**Table 1**

Results of thermal analysis by differential scanning calorimetry at 2 and 10 K/min compared with temperatures observed by neutron diffraction and for the previous study of Kim et al. [9].

Sample	$T_g$	$T_{x1}$	$T_{x2}$	$T_{m1}$	$T_{m2}$	$T_m$
DSC—this study (2 K/min)	555	608	749	810	845	955
Neutron—this study (2 K/min)		610	724	814		
DSC—this study (10 K/min)	575	628	765	825	865	
Prev. [9] (10 K/min)	621	668	776	813		948

previous experiments performed by other groups [9], the results are rather in good agreement with previous results. Fig. 1 shows the DSC trace recorded at 2 K/min, the glass transition temperature is not well marked and there is a continuous endothermic reaction starting around 555 K. A first crystallization event (exothermic) appears at  $T_{x1}$  = 608 K with low intensity and a broad temperature range. A second crystallization event (exothermic) appears at  $T_{x2}$  = 749 K with a sharper peak. A first endothermic reaction occurs at  $T_{m1}$  = 810 K (low intensity), a second endothermic event occurs at  $T_{m2}$  = 845 K (low intensity) and the full melting occurs at  $T_m$  = 955 K. In the previous studies [9], the  $T_{x1}$  and  $T_{x2}$  were observed, but  $T_{m1}$  was also considered as a crystallization event, full melting was observed at 948 K.

In situ neutron diffraction experiments have been done on 2 samples of the same batch and with 2 heating profiles. The first heating treatment was done at a constant speed of 2 K/min and a diffraction pattern was recorded continuously during the temperature change every 5 min (each neutron pattern has a mean temperature value during a 10 K change) up to 930 K, then cooling down at room temperature. The second heating treatment was a constant heating at 2 K/min up to  $T_g + 30$ , then a dwell at this temperature until crystallization was not evolving, then cooling down at room temperature.

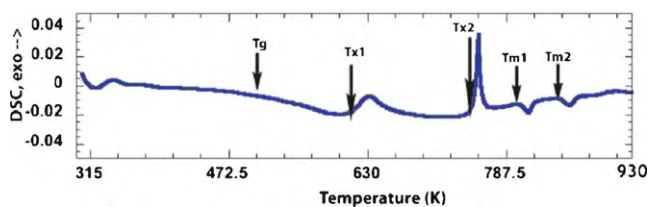


Fig. 1. DSC trace obtained from the 3 mm sample at 2 K/min with notation of the thermic events.

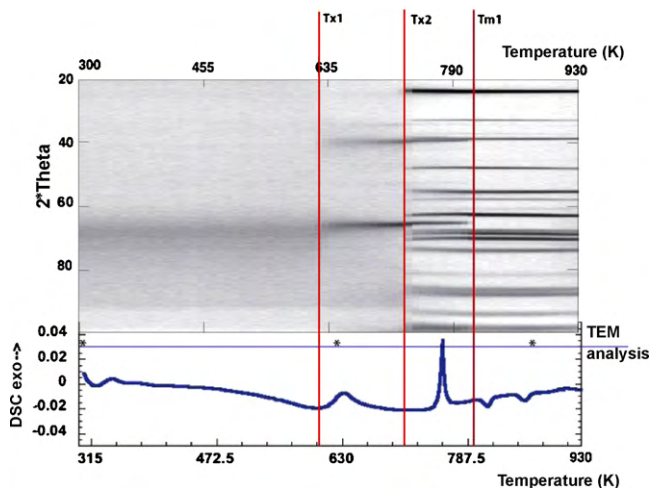


Fig. 2. Neutron diffraction pattern evolution with temperature compared with the DSC analysis at 2 K/min.

**Table 2**

Results of the neutron phase refinement of the sample heated at 930 K, and then cooled down at 300 K.

Atom	C14 Laves phase, hexagonal P63/mmc, $a = 5.228(1)\text{Å}$ , $c = 8.629(2)\text{Å}$			Occ.
Zr (4f)	1/3	2/3	$Z = 0.065(1)$	0.1666
Ti (2a)	0	0	0	0.067
Cu (2a)				0.067
Ti (6h)	$x = 0.836(3)$	$x$	$x$	0.113
Ni (6h)				0.137
Atom	Big cube phase, cubic Fd3m, $a = 10.871(1)\text{Å}$			Occ.
Zr (48f)	$X = 0.192(1)$	0	0	0.027
Ti (48f)				0.223
Zr (16d)	5/8	5/8	5/8	0.051
Ti (16d)				0.033
Cu (32e)	$x = 0.943(1)$	$x$	$x$	0.106
Ni (32e)				0.061

Fig. 2 shows the constant heating experiment such as the  $x$ -axis is the  $2\theta$  diffraction angle,  $y$ -axis is the time (during temperature change) and the  $z$ -axis is the neutron counts intensity. At the beginning of the experiment, the characteristic diffraction pattern of an amorphous compound with short-range order (bump maximum at  $2\theta = 68^\circ$ ;  $d = 2.514\text{Å}$ ) is observed. At 610 K (608 K in DSC experiment), some new peaks appear at  $2\theta = 39.34^\circ$  and  $65.54^\circ$  corresponding to  $d$  spacings 3.785 and 2.340 Å respectively, these peaks are diffuse at the beginning corresponding certainly to very tiny crystals, then sharper with time and temperature increasing. With only 2 diffraction peaks it is difficult to ascertain the nature of the new formed phase, but we can exclude some hypothesis, in particular  $\alpha$ - or  $\beta$ -Ti, which did not present a peak at  $d = 3.785\text{Å}$ . In the same way the icosahedral phase often observed in phases with beryllium presents a double peak around  $d = 2.34\text{Å}$ . In simple binary phases, only the  $\text{TiBe}_2$  (face centered cubic,  $a = 6.45\text{Å}$ ) phase presents 2 peaks close to the observed peaks, by refining the cell parameter, the value  $a = 6.603\text{Å}$  has been determined. It could be explained by a partial replacement of Ti by a bigger atom such as zirconium. However the  $\text{ZrBe}_2$  compound is hexagonal, so only partial replacement must be assumed. This mixed phase (Ti,Zr)Be<sub>2</sub> phase has different stability parameters than  $\text{TiBe}_2$ .

At  $T = 724\text{K}$ , new peaks appear and the main phases agreeing with peak positions are an hexagonal C14 phase with cell parameters  $a = 5.25\text{Å}$  and  $c = 8.65\text{Å}$  at high temperature, and a cubic  $\text{Zr}_2\text{Ni}$  phase with  $a = 11.00\text{Å}$  at high temperature. These phases are present at all temperatures up to 930 K and also after cooling at room temperature. The temperature of the crystallization event is observed well below the temperature observed during the DSC experiment (749 K). We have no explanation for this temperature difference.

The last observation of this constant speed experiment is the disappearance of the primary crystallization phase (Ti,Zr)Be<sub>2</sub> at  $T_{m1} = 814\text{K}$ , which is in agreement with the DSC experiment ( $T_{m1} = 810\text{K}$ ). After heating at 930 K (just before melting), no other phenomena is observed, so the sample was cooled at room temperature and these data used to perform a profile refinement. The data refinement is reported in Table 2 and Fig. 3, using a C14 hexagonal model for one phase and the big cube phase model for the other one. Cell parameters, occupation factors of the various sites and their atomic positions (when variables) were refined and the result are reported in Fig. 3. The refinement quality factors were respectively 6.7%, 8.9% and 3.5% for C14 phase, cubic phase and full profile. For the C14 phase, it corresponds to the formula  $\text{Zr}_{1.0}\text{Ti}_{1.08}\text{Ni}_{0.82}\text{Cu}_{0.10}$  or  $\text{Zr}(\text{Ti},\text{Ni},\text{Cu})_2$  or  $\text{Zr}_{33.3}\text{Ti}_{35.9}\text{Ni}_{27.3}\text{Cu}_{3.4}$  and it represents 92% of phase quantity. This phase has been previously described by Waterstrat [17] as  $\text{ZrTiNi}$  with  $a = 5.205\text{Å}$  and  $c = 8.476\text{Å}$ . The cell parameters as measured in this experiment are

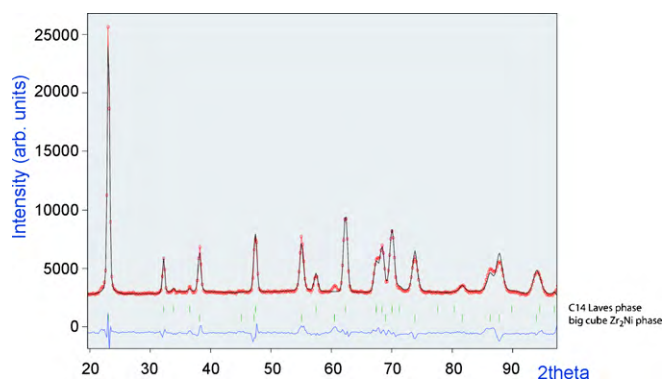
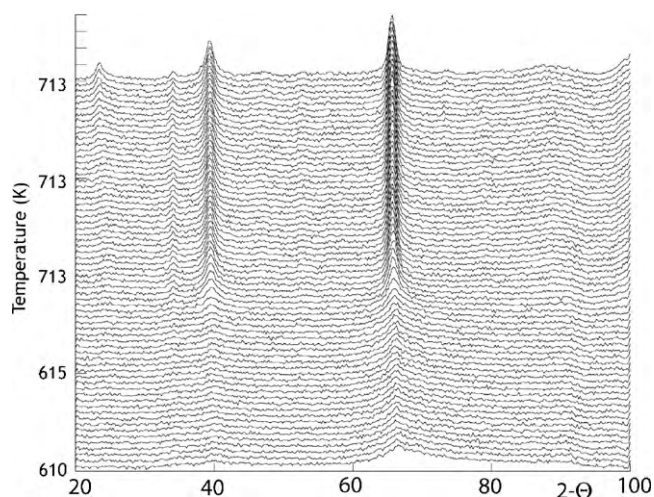


**Fig. 3.** Neutron 2-phases refinement of the sample heated at 930 K, then cooled down at 300 K. Dots are the experimental points, line is the intensity fit, vertical ticks are for the C14 Laves phase and the big cube phase, line below is the difference between observed and calculated neutron intensity.

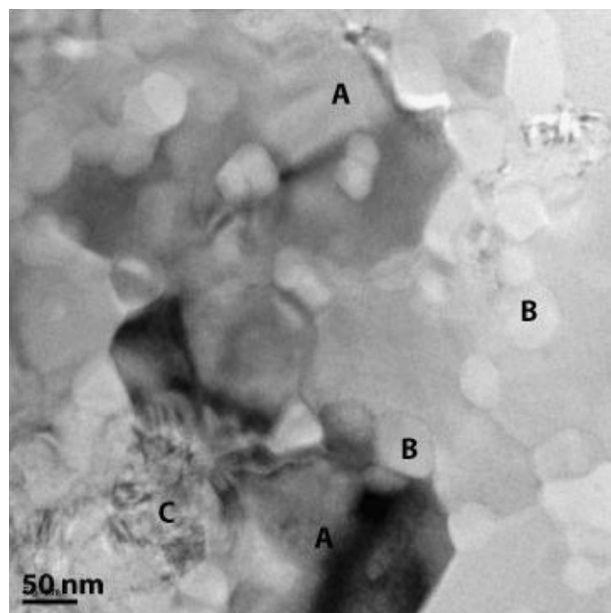
slightly bigger due to a different site occupation. For the “Big cube” phase, it corresponds to the formula  $\text{Ti}_{1.536}\text{Zr}_{0.464}\text{Ni}_{0.364}\text{Cu}_{0.636}$  or  $(\text{Ti,Zr})_2(\text{Ni,Cu})$  or  $\text{Ti}_{51.2}\text{Zr}_{15.5}\text{Ni}_{12.1}\text{Cu}_{21.2}$  and it represents 8% of phase quantity. This phase has often been reported in Zr-based BMG as the primary crystallization phase with cell parameter in the range 11.95–12.09 Å [18]. All lines are indexed and calculated with a fairly good agreement.

Fig. 4 shows the static heating experiment at 713 K (before the second crystallization event). At the beginning of the experiment, the characteristic diffraction pattern of an amorphous compound with short-range order (bump maximum at  $2\theta = 68^\circ$ ;  $d = 2.514$  Å) is observed, like in the first experiment. At 610 K the new peaks of the cubic  $(\text{Ti,Zr})\text{Be}_2$  phase appear and are becoming finer with time evolution, meaning growing of crystals. After 150 min at this temperature, new peak appears close to  $2\theta = 24^\circ$ , corresponding to the main line of the big cube phase. The big cube phase is the second crystallization product to be formed after the  $(\text{Ti,Zr})\text{Be}_2$  phase.

An annealed sample at  $T = 790$  K for 5 min has been studied by TEM and is presented in Fig. 5. Three different kinds of crystals are observed: crystals (A) have a regular shape with 200 nm size, they appear in black or grey color, crystals (B) have also a regular shape with 50 nm size, they appear in a white color, crystals (C) have a “flower-” or “feather-” like shape, very irregular and 250 nm in size. The chemical mean analysis is reported in Table 3. There is a good agreement between neutron chemical analysis and EDS



**Fig. 4.** 3-dimensional plot of the neutron annealing experiment at  $T = 713$  K. x-axis is the  $2\theta$  diffraction angle, y-axis is the temperature (time) evolution and z-axis is the neutron intensity.



**Fig. 5.** Bright field TEM image of an annealed sample at  $T = 790$  K for 5 min. Three different crystals family are observed. (A) Large faceted crystals, (B) small round crystals, and (C) “feather-” or “flower-” like crystals.

**Table 3**

Results of the phase percentages obtained by electron microscopy EDS chemical analysis and by neutron diffraction refinement.

Elements Phases	Zr (at%)	Ti (at%)	Cu (at%)	Ni (at%)	Be (at%)
Crystals (A) (EDS)	36.9	34.6	15.2	13.2	
C14 laves phase—neutron	33.3	35.9	3.4	27.3	
Crystals (B) (EDS)	20.4	60.9	8.3	10.4	
Big cube phase—neutron	15.5	51.2	21.2	12.1	
Crystals (C) (EDS)	54.2	45.0	0.5	0.3	
Ti(Zr)Be <sub>2</sub> cubic phase—neutron	16.6	16.6	0	0	66.6

chemical analysis concerning the elements phase content. EDS did not analyze beryllium in the  $(\text{Ti,Zr})\text{Be}_2$  structure, as it has a too low number of electrons and the chemical formula is calculated only on the elements that are observed. But we can consider it is the good phase as there is no copper or nickel inside and that the peaks of the  $\alpha$ -Ti or  $\beta$ -Ti phase are not observed. The formation of the  $(\text{Ti,Zr})\text{Be}_2$  phase as primary crystallization phase (PCP) is in agreement with previous primary crystallization studies of BMG containing beryllium phase. We have observed during the crystallization of  $\text{Zr}_{46.75}\text{Ti}_{8.25}\text{Cu}_{7.5}\text{Ni}_{10}\text{Be}_{27.5}$  phase the formation of  $\text{ZrBe}_2$  and a quasicrystalline phase [19] as PCP and whose TEM images are very similar in shape and size. Depending on the synthesis conditions during the glass formation (sample diameter, cooling rate, and oxygen presence), different phases can be formed because of the different atomic structures (short-range order) possible in the glass state. It is why the observations of Kim [9] and Kou [12] of a quasicrystalline phase as PCP may be also the result of the BMG synthesis process, different from our samples.

#### 4. Conclusion

By coupled experiments by in situ neutron diffraction, DSC and TEM/EDS, we have evidenced the phases formed during heating or annealing the  $(\text{Ti}_{40}\text{Zr}_{25}\text{Ni}_8\text{Cu}_9\text{Be}_{18})$  bulk metallic glass. During the primary crystallization, a cubic  $(\text{Ti,Zr})\text{Be}_2$  phase is formed, this phase is unstable and decomposes at higher temperature. The second crystallization products, which are very

stable up to full melting, are at 92% a C14 hexagonal Laves phase  $Zr_{1.0}Ti_{1.08}Ni_{0.82}Cu_{0.10}$  or  $Zr(Ti,Ni,Cu)_2$ , and at 8% a big cube phase,  $Ti_{1.536}Zr_{0.464}Ni_{0.364}Cu_{0.636}$  or  $(Ti,Zr)_2(Ni,Cu)$ . We have not evidenced the formation of an icosahedral phase as in previous studies, but this may due to a different synthesis process. Further measurements of mechanical properties are done on these materials and will be compared to other materials prepared with a different process to see if the PCP has an influence on mechanical properties.

## References

- [1] T. Zhang, A. Inoue, *Trans. Mater. JIM* 40 (1999) 301.
- [2] T. Zhang, A. Inoue, *Mater. Sci. Eng. A* 304–306 (2001) 771.
- [3] C. Ma, S. Ishihara, H. Soejima, N. Nishiyama, A. Inoue, *Mater. Trans.* 45 (2004) 1802.
- [4] H. Men, S. Pang, A. Inoue, T. Zhang, *Mater. Trans.* 46 (2005) 2218.
- [5] G. Wang, Y.H. Liu, P. Yu, D.Q. Zhao, M.X. Pan, W.H. Wang, *Appl. Phys. Lett.* 89 (2006) 251909.
- [6] K.B. Kim, J. Das, S. Venkataraman, S. Yi, J. Eckert, *Appl. Phys. Lett.* 89 (2006) 71908.
- [7] S.L. Zhu, X.M. Wang, F.X. Qin, A. Inoue, *Mater. Trans.* 48 (2007) 163.
- [8] S.L. Zhu, X.M. Wang, F.X. Qin, M. Yoshimura, A. Inoue, *Mater. Trans.* 48 (2007) 2445.
- [9] Y.C. Kim, W.T. Kim, D.H. Kim, *Mater. Sci. Eng. A* 375–377 (2004) 127.
- [10] J.M. Park, H.J. Chang, K.H. Han, W.T. Kim, D.H. Kim, *Scripta Mater.* 53 (2005) 1.
- [11] J.N. Mei, J.S. Li, H.C. Kou, J.L. Soubeyroux, H.Z. Fu, L. Zhou, *J. Alloys Compd.* 467 (2009) 235.
- [12] H.C. Kou, J. Wang, H. Chang, B. Tang, J.S. Li, R. Hu, L. Zhou, *J. Non-Cryst. Sol.* 355 (2009) 420.
- [13] H.C. Kou, J. Wang, B. Tang, X.F. Gu, R. Hu, J.S. Li, L. Zhou, *J. Alloys Compd.* 479 (2009) L22.
- [14] J. Wang, H.C. Kou, J.S. Li, X.F. Gu, L.Q. Xing, L. Zhou, *J. Alloys Compd.* 479 (2009) 835.
- [15] W.F. Ma, H.C. Kou, J.S. Li, H. Chang, L. Zhou, *J. Alloys Compd.* 472 (2009) 214.
- [16] J. Rodriguez-Carvajal, *Physica B* (1993) 192.
- [17] R.M. Waterstrat, *J. Alloys Compd.* 179 (1992) L33.
- [18] M. Barico, S. Spriano, I. Chang, M.I. Petrzhik, L. Battezzati, *Mater. Sci. Eng. A* 304–306 (2001) 305.
- [19] B. Van De Moortèle, T. Epicier, J.L. Soubeyroux, J.M. Pelletier, *Phil. Mag. Lett.* 84 (2004) 245.